


 Cite this: *Phys. Chem. Chem. Phys.*, 2025, 27, 25276

 Received 8th August 2025,  
 Accepted 5th November 2025

DOI: 10.1039/d5cp03040d

[rsc.li/pccp](https://rsc.li/pccp)

# Evaluating the impact sensitivity of energetic materials using inelastic neutron scattering and low frequency THz-Raman spectroscopies

 Adam A. L. Michalchuk,<sup>id</sup>\*<sup>ab</sup> Carole A. Morrison,<sup>id</sup>\*<sup>c</sup> Colin R. Pulham<sup>id</sup><sup>c</sup> and Svemir Rudić<sup>id</sup><sup>d</sup>

**New methods that are suitable for the rapid screening of energetic material (EM) impact sensitivity are needed for the high-throughput discovery of EMs. We here demonstrate a proof-of-concept experimental vibrational spectroscopy (inelastic neutron scattering spectroscopy and low-frequency THz-Raman spectroscopy) study that has promise in this regard. Specifically, we show that a modified version of the vibrational up-pumping model can be applied to experimental vibrational spectroscopy data, to provide a screening tool to rank the impact sensitivities of EMs. We demonstrate the potential of this method on a preliminary set of EMs – CL-20, HMX, FOX-7, NTO, and TATB – with our findings indicating that portable spectroscopic probes could become suitable for the contactless and non-destructive evaluation of milligram quantities of EMs, expediting the design and discovery of new EMs. We expect such analyses could become useful for ensuring novel EMs are safe to handle before performing larger scale sensitivity tests.**

EM properties, most notably their sensitivity to initiation by mechanical impact. Correspondingly, new EMs must be synthesised in gram-scale quantities without prior knowledge of their sensitivity, and then tested. Not only does this approach delay progress of EM technologies, but it poses significant risk to the safety of those involved in the development and handling of EMs.

To expedite EM discovery, and mitigate the associated risk to safety, the community has sought methods to predict the impact sensitivity of EMs, with the aim of evaluating EMs *in silico*. A common approach has been to fit empirical equations to large datasets of EM properties (including *via* machine learning),<sup>1–6</sup> targeting parametric correlations with impact sensitivity. These methods are particularly well suited to screen large datasets very quickly and provide powerful routes for screening purposes. However, as these models are not based on a physical model of reactivity, their use to identify the chemical origins for EM sensitivity – and hence guide the design of new EMs – is limited.

In this regard, another strand of research has focused on developing mechanistic models for EM sensitivity, often through linking reactivity indicators (bond dissociation energies,<sup>7</sup> charge density distribution,<sup>8</sup> *etc.*) against sensitivity, usually based on properties of isolated molecules. Whilst useful for linking reactivity to molecular features, these methods are unable to describe why different crystal forms of an EM (polymorphs<sup>9</sup> and cocrystals<sup>10</sup>) often exhibit different impact sensitivity. Capturing this behaviour requires a more complete picture of impact sensitivity that accounts for behaviour in the solid state.

A promising effort in this direction is based on the concept of phonon energy transfer,<sup>11–13</sup> wherein the mechanical energy from an impact or shock couples to low-frequency phonons of a crystal, and scatters (up-pumps) into higher frequency phonons. Once the energy localises in molecular degrees of freedom, it distorts the molecule and causes bond dissociation.<sup>14,15</sup> This is the initiation step of the explosive reaction. Using this concept, both our group<sup>16,17</sup> and others<sup>18,19</sup> have shown that

## Introduction

Energetic materials (EMs; explosives, propellants, pyrotechnics and gas generators) are characterised by their ability to rapidly release energy in response to external stimuli such as mechanical impact. This behaviour makes EMs essential in many technologies, from mining and demolition through to defence applications. With growing pressure to improve the safety and reduce the environmental impact of EMs, there are considerable efforts being devoted to the design of new EMs. Unfortunately, there is limited understanding of how to target critical

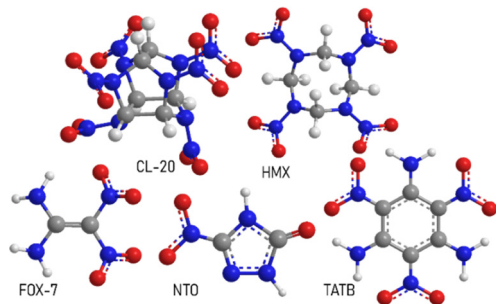
<sup>a</sup> School of Chemistry, University of Birmingham, Birmingham, B15 2TT, UK.  
 E-mail: a.a.l.michalchuk@bham.ac.uk

<sup>b</sup> Federal Institute for Materials Research and Testing (BAM), Richard-Willstätter Str 11, 12489, Berlin, Germany

<sup>c</sup> EaStCHEM School of Chemistry, University of Edinburgh, Edinburgh, EH9 3FJ, UK. E-mail: c.a.morrison@ed.ac.uk

<sup>d</sup> ISIS Neutron and Muon Source, STFC Rutherford Appleton Laboratory, Didcot, OX11 0QX, UK





**Scheme 1** Molecular structures for the test set of EMs studied here. Molecules include CL-20 (hexanitrohexaazaisowurtzitan), HMX (octahydro-1,3,5,7-tetranitro-1,3,5,7-tetrazocine), FOX-7 (diamino-dinitro-ethene), NTO (nitrotriazolone), and TATB (triamino-trinitrobenzene). Atoms are coloured as: oxygen (red), nitrogen (blue), carbon (grey), hydrogen (white).

phonon energy transfer rates based on *ab initio* phonon frequencies offer predictive capability to assess EM impact sensitivity. Moreover, with this up-pumping model we can predict, and therefore rank, the relative impact sensitivities of different EM crystal structures, including polymorphs<sup>20,21</sup> and cocrystals.<sup>22</sup>

The foundation of this predictive model is the input of a set of simulated phonon frequencies. However, one might expect that phonon frequencies obtained by any appropriate technique could be suitable for this model, for example from vibrational spectroscopy.<sup>11</sup> If true, a combination of our phonon up-pumping model with readily measurable experimental vibrational spectra could offer a new non-destructive, small-scale, and rapid tool to screen EM sensitivity. Crucially, as this approach would rely on having only enough material to record a vibrational spectrum, it could facilitate the high-throughput experimental design of new EMs. Simultaneously, this method would also make EM testing significantly safer, as it would provide a route to screen EM sensitivity prior to the need to synthesise larger quantities (typically multiple grams) for drop-weight impact-sensitivity testing.

To explore this possibility, herein we investigate whether experimental vibrational spectra can be used for sensitivity

predictions using a small, proof-of-concept family of EMs including  $\epsilon$ -CL-20,  $\beta$ -HMX,  $\alpha$ -FOX-7,  $\alpha$ -NTO, and TATB, Scheme 1. These EMs exhibit a wide range of structure types and impact sensitivities (from literature:  $\epsilon$ -CL-20, *ca.* 2 J;  $\beta$ -HMX, *ca.* 10 J;  $\alpha$ -FOX-7, *ca.* 30 J;  $\alpha$ -NTO, > 50 J; and TATB, > 120 J),<sup>7,23,24</sup> providing a range of responses against which to evaluate a successful proof-of-concept study.

Our study makes use of inelastic neutron scattering spectroscopy (INS), as available at the ISIS Neutron and Muon facility, and a lab-based portable low frequency Raman spectrometer which enables the measurement of frequencies in the THz range. THz frequency spectroscopies are important tools for material diagnostics,<sup>25</sup> where they have been demonstrated to successfully identify the structure and content of materials. For example THz frequency spectroscopy has been used to assess the water content in biological materials,<sup>26</sup> to characterise the composition of minerals,<sup>27</sup> and to monitor transformations between solid forms (*i.e.*, polymorphs).<sup>28,29</sup> Recently, the EM community has also recognised THz frequency spectroscopies as potential tools for the detection and identification of EMs.<sup>30,31</sup> Our study therefore adds a new dimension to the range of opportunities enabled by this low frequency vibrational spectroscopy for the study of materials and, specifically, EMs.

## Background theory

A full description of the up-pumping theory can be found elsewhere,<sup>16,32</sup> and only a brief summary is given here.

The vibrational up-pumping model describes the redistribution of vibrational (kinetic) energy according to,

$$\tau \propto |V^{(3)}| \delta(\omega_3 - \omega_2 - \omega_1) \quad (1)$$

where  $|V^{(3)}|$  is the strength of scattering between a set of three phonon modes  $\omega_3$ ,  $\omega_2$ , and  $\omega_1$ , which conserve energy as imposed by the Dirac delta function. Momentum conservation is taken as implicit.

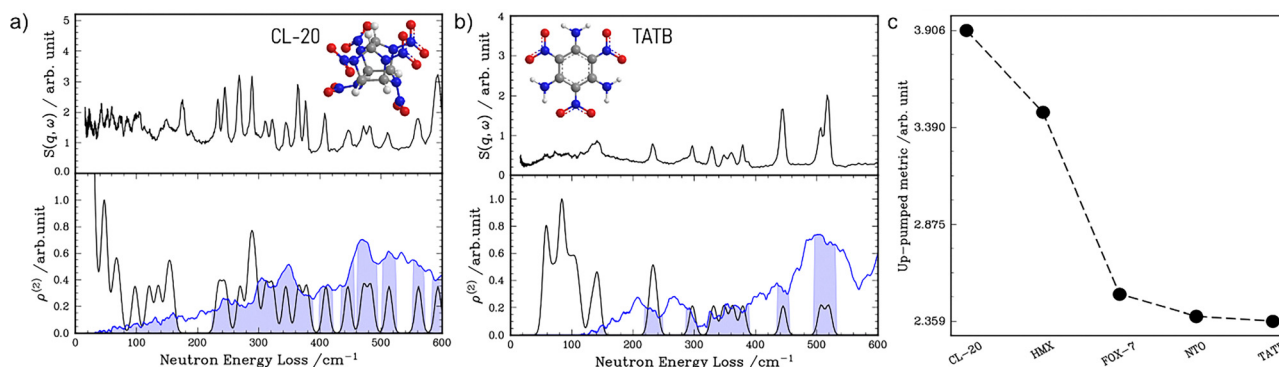


**Fig. 1** Inelastic neutron scattering (INS) spectra as a screening tool for EM impact sensitivity prediction based on the up-pumping model (see SI, S3 for a worked example). Shown for (a)  $\epsilon$ -CL-20 and (b) TATB, the (top image) background-subtracted INS spectra measured for polycrystalline samples, (bottom image) the pseudo phonon density of states  $g'(\omega)$  generated from the INS data (black), alongside the two-phonon density of states (blue,  $\rho^{(2)}$ ) and its projection onto  $g'(\omega)$  (shaded areas). (c) The up-pumping metric obtained from the integration of  $\rho^{(2)}$  projected onto  $g'(\omega)$ . Note that experimental sensitivity follows as  $\epsilon$ -CL-20 >  $\beta$ -HMX >  $\alpha$ -FOX-7 >  $\alpha$ -NTO > TATB.



To bypass the extreme computational costs associated with the calculation of  $|V^{(3)}|$ , models have traditionally adopted the average anharmonic approximation,<sup>33</sup> which enables the order-of-magnitude of  $|V^{(3)}|$  to be approximated based on the type of vibrational modes involved. The larger the number of external vibrational modes (usually characterised by  $\omega < 200 \text{ cm}^{-1}$  with the upper bound defined as  $\Omega_{\text{max}}$ ) involved in the scattering process, the stronger the scattering strength. This approximation leads to the set-up of a three-step up-pumping model: (1) excitation and equilibration of energy across the external vibrational modes with  $\omega < \Omega_{\text{max}}$ ; (2) the transfer of energy into vibrations with intermediate frequencies of  $\Omega_{\text{max}} < \omega < 2\Omega_{\text{max}}$ ; and (3) the final transfer and localisation of energy into high frequency molecular vibrations (with frequency up to  $3\Omega_{\text{max}}$ ). Once energy has been transferred through these three steps, we take the integral of the up-pumped energy that is resonant with the fundamental frequencies of the EM as an indication for the impact sensitivity. It follows from the above discussion that sensitivity prediction based on the phonon up-pumping model only requires a set of vibrational frequencies as input.

## Results and discussion

Within the framework of the phonon up-pumping model, there are two major challenges with using experimentally-derived data: (1) the model requires low-frequency vibrational data, which are typically inaccessible, and (2) many vibrational bands are not observed because of restrictions imposed by the relevant quantum mechanical selection rules.

An immediate route to overcoming both challenges is to obtain inelastic neutron scattering (INS) spectra, which we have measured for all our model EMs (see Fig. 1(a), (b) and SI, S3). Immediate inspection of the INS spectra does suggest a qualitative correlation between the spectra and impact sensitivity. The more sensitive compounds ( $\epsilon$ -CL-20 and  $\beta$ -HMX) have markedly denser INS spectra as compared with the less sensitive materials (NTO and TATB). Importantly, the intensities of INS spectra are proportional to the (neutron scattering strength-weighted) phonon density of states. Moreover, the neutron scattering strength of a given EM is proportional to the relative proportions of C, H, N, O atoms that it contains. As this proportion is approximately the same for each of the EMs in Scheme 1 (e.g. hydrogen content: CL-20 17%, HMX 28%, FOX-7 28%, NTO 18% and TATB 25%), we make the crude approximation that the neutron scattering weighting is also roughly equivalent for this set of materials. With this approximation, we can use the INS spectra as inputs for the phonon density of states  $g(\omega)$  within our up-pumping model.

To perform up-pumping calculations using experimental INS spectra (see worked example in SI, S3), all data were first background subtracted, and the two-phonon density of states were generated,

$$\rho^{(2)} = \int \delta(\omega_3 - (\omega_1 + \omega_2))g(\omega_1)g(\omega_2)d\omega_1d\omega_2 \quad (2)$$

The curve of  $\rho^{(2)}$  is indicative of the amount of energy that is transferred through three-phonon scattering processes

(i.e. first-order anharmonicity) into higher frequency phonon modes. However, the EMs can only absorb up-pumped energy that is resonant with existing vibrational states, which we approximate by projecting the  $\rho^{(2)}$  (normalized to unity) onto  $g(\omega)$ . When using the INS spectra as the input data for  $g(\omega)$ , however, it proved numerically challenging to avoid projection onto the residual background features of the spectra.

To overcome this issue, we generated a pseudo density of states  $g'(\omega)$  by convoluting a Gaussian function (width  $5 \text{ cm}^{-1}$ ) with the Dirac delta functions centred on each identified peak, onto which  $\rho^{(2)}$  was projected (see Fig. 1(a) and (b) and SI, S3). Peak identification was automated using SciPy's wavelet transform algorithm and the outputs were manually verified to ensure all spectra peaks were identified.<sup>34</sup> Computed vibrational frequencies derived from density functional theory (see SI, S2) were also used as a guide, when required, to differentiate between weak bands and background noise. We note that only the spectral coverage of  $g'(\omega)$  is important, not its intensity, as this determines the amount of  $\rho^{(2)}$  being absorbed.

The final metric of impact sensitivity was obtained by integrating the projection of  $\rho^{(2)}$  across the region  $\Omega_{\text{max}}-3\Omega_{\text{max}}$ , normalized by the integration range.  $\Omega_{\text{max}}$  denotes the highest frequency lattice vibration, and integration to  $3\Omega_{\text{max}}$  accounts for all allowed 3-phonon scattering processes (see details in ref. 16). For the INS data, we selected  $\Omega_{\text{max}}$  values to be consistent with our calculated values (see details in ref. 16), adjusted for shifts observed in the experimental data:  $\epsilon$ -CL20 ( $195 \text{ cm}^{-1}$ ),  $\beta$ -HMX ( $200 \text{ cm}^{-1}$ ),  $\alpha$ -FOX7 ( $185 \text{ cm}^{-1}$ ),  $\alpha$ -NTO ( $200 \text{ cm}^{-1}$ ), and TATB ( $150 \text{ cm}^{-1}$ ).

Performing this up-pumping procedure for all the INS datasets leads to a clear trend in EM sensitivity, Fig. 1(c). For the most sensitive EMs  $\epsilon$ -CL-20 and  $\beta$ -HMX, most of the up-pumped density is resonant with the material's fundamental frequencies, indicating effective vibrational energy transfer and high sensitivity to mechanical impact. In contrast, for the lowest sensitivity materials  $\alpha$ -NTO and TATB, very little of the up-pumped energy is resonant with the fundamental frequencies, indicating the opposite. Though the variation in sensitivity response obtained from the up-pumping model based on INS data is not as stark as that based on DFT calculated frequencies<sup>16</sup> (presumably because of the additional approximations made in the former), analysis based on INS data clearly provides a facile basis for differentiating between sensitive and insensitive materials.

Our ability to evaluate the relative impact sensitivities of the model EMs using INS spectroscopy is reassuring. However, access to this method requires large-scale specialised facilities and  $>1 \text{ g}$  of material. INS is by no means suited for on-site laboratory screening and does not alleviate the safety hazard associated with novel EM development. For this reason we next turned our attention to an emerging laboratory probe, the THz-Raman spectrometer,<sup>35</sup> which uses new notch filter technology to provide access to low-frequency Raman shifts within  $\sim 5 \text{ cm}^{-1}$  of the excitation wavelength. While THz-Raman spectroscopy does give access to the low-frequency region required to solve the first challenge posed above, it is a Raman



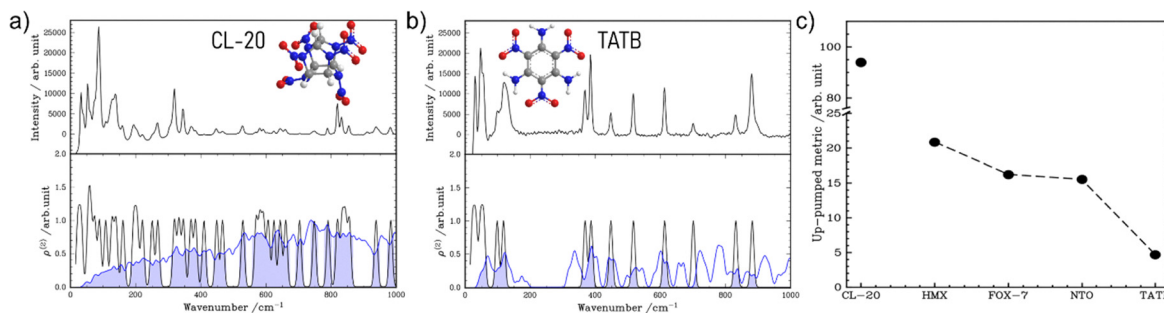


**Fig. 2** THz-Raman spectra as a screening tool for EM impact sensitivity using the up-pumping model (see SI, S4 for a worked example). (a) and (b) For CL-20 and TATB, the (top) background subtracted THz-Raman spectra measured on powder samples, (bottom) the pseudo density of states  $g'(\omega)$  generated from THz-Raman spectra (black), alongside the two-phonon density of states (blue,  $\rho^{(2)}$ ) and its projection onto  $g'(\omega)$  (shaded). (c) The up-pumping metric obtained from the integration of  $\rho^{(2)}$  projected onto  $g'(\omega)$ . Note experimental sensitivity follows as  $\epsilon$ -CL-20 >  $\beta$ -HMX >  $\alpha$ -FOX-7 >  $\alpha$ -NTO > TATB.

scattering technique and is thus restricted to measuring Raman-active bands. We were therefore uncertain if sufficient vibrational bands could be measured in each EM for the vibrational up-pumping model to operate correctly.

To explore the suitability of experimental THz-Raman spectra as a screening tool for IS prediction, we collected room-temperature spectra on polycrystalline samples of our model EMs (see Fig. 2 and SI, S4 for worked example). As expected, all the spectra comprise somewhat fewer vibrational bands as compared with the INS spectra. We note also that, unlike our INS spectra, the intensity of the THz-Raman data is not proportional to the density of states, and therefore require some modification to our phonon up-pumping model.

Our method for processing the experimental THz-Raman data follows the same procedure as for the INS data, except that

the initial  $g(\omega)$  are replaced by  $g'(\omega)$ , *i.e.*  $\rho^{(2)}$  is first generated using  $g'(\omega)$ , and is subsequently projected back onto  $g'(\omega)$  to calculate the total amount of transferred energy. The procedure is given in full in SI, S4 and examples are shown in Fig. 2 for the most sensitive ( $\epsilon$ -CL-20) and least sensitive (TATB) compounds in our study. We note that the choice of peak width when generating  $g'(\omega)$ , which we set to  $5\text{ cm}^{-1}$  for all peaks throughout the data sets for all molecules, will have particular influence on the up-pumping metric calculated in this way, as it influences both the shape of  $\rho^{(2)}$  and its subsequent projection onto  $g'(\omega)$ . Our analysis, SI, S4, shows that, while numerical values do alter depending on our choice of peak width, with the exception of unphysically small Gaussian broadening, the relative ordering of our sensitivity predictions is invariant to the choice of peak width.

By following this procedure, and subsequently integrating the projection of  $\rho^{(2)}$  onto  $g'(\omega)$  we obtain a normalised quantification for the amount of  $\rho^{(2)}$  that is effectively absorbed by the EM, thereby resulting in chemical initiation. Note that the final integration is performed over the up-pumping window of  $\Omega_{\text{max}}$  to  $3\Omega_{\text{max}}$ , with values of  $\Omega_{\text{max}}$  for the THz-Raman data:  $\epsilon$ -CL20 ( $200\text{ cm}^{-1}$ ),  $\beta$ -HMX ( $200\text{ cm}^{-1}$ ),  $\alpha$ -FOX7 ( $185\text{ cm}^{-1}$ ),  $\alpha$ -NTO ( $215\text{ cm}^{-1}$ ), and TATB ( $140\text{ cm}^{-1}$ ).

When this procedure is performed for each of the model systems, we observe a strong, albeit qualitative, trend between the up-pumped density and the experimental impact sensitivity, as shown in Fig. 2(c). As observed for the INS data, the proportion of up-pumped energy absorbed by the sensitive materials ( $\epsilon$ -CL-20 and  $\beta$ -HMX) is significantly higher than for the low-sensitivity materials ( $\alpha$ -NTO and TATB). Our findings suggest that, although it may not currently be possible to use spectroscopic data to differentiate decisively between materials of similar impact sensitivity, it should be possible to distinguish materials of notably different sensitivity. This THz-Raman approach is particularly useful as a method for the rapid evaluation of impact sensitivity using only very small quantities (mg) of a novel material, thereby informing the precautions that must be taken for its safe handling. It is also non-destructive, in contrast with the current methods to deduce impact initiation, such as the BAM fall hammer test.

Although initially one might expect that the loss of Raman-inactive bands in the THz-Raman spectrum would make it impossible to perform up-pumping calculations, this clearly

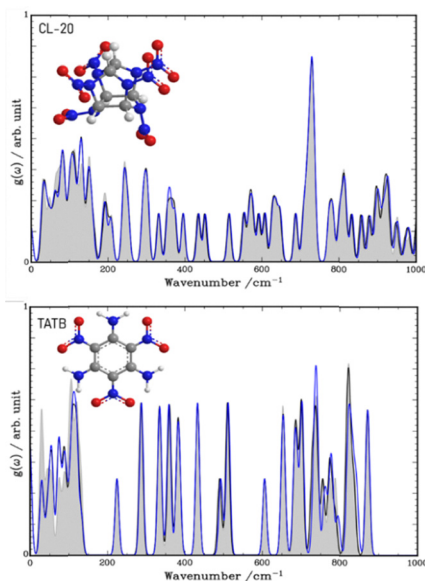


**Fig. 3** The DFT simulated phonon density of states,  $g(\omega)$ , for (top) CL-20 and (bottom) TATB. Simulations were performed at PBE-D3 (black) and PBE-D4 (blue) levels of theory. The  $g(\omega)$  were additionally calculated (shaded area) using only the Raman-active vibrational bands. In all cases  $g(\omega)$  were prepared using a Gaussian broadening of  $\pm 5\text{ cm}^{-1}$ . A full set of simulated data are given in SI, S2.



is not the case. We can understand this by considering DFT-simulated vibrational spectra for the selected compounds, Fig. 3 and SI, S2. Through mode-symmetry analysis of the calculated eigenvectors, the phonon density of states can be recast to omit the Raman-inactive bands. The comparison shows that for the EMs studied here there is very little difference in the overall structure of the phonon density of states, affecting only the absolute intensity of the density of states with little alteration of the coverage of frequency space. In turn this means that, by omitting the Raman-inactive bands, we do not significantly change the ability of the density of states to absorb energy from up-pumping (*i.e.* the projection of  $\rho^{(2)}$  onto  $g(\omega)$ ).

## Conclusions

Using a small proof-of-concept set of EMs we demonstrate that, with minor modifications, it is possible to perform a phonon up-pumping calculation using as input either the high-resolution data obtained from INS spectroscopy or low-frequency data obtained from THz-Raman spectroscopy. For both data sets, our model provides a qualitative trend consistent with the experimental impact sensitivities of a set of EMs. Given that some of the pioneering work on vibrational up-pumping in the 1990s sought to use experimentally derived data as input,<sup>11,36</sup> but were restricted by low quality instrumental resolution at the time, it is gratifying to see how advances in both spectroscopic measurements and the theoretical framework of the up-pumping model are beginning to make this early hypothesis a reality.

Whilst we have only been able to test our spectroscopy-based up-pumping model on a small set of EMs, our results suggest that an up-pumping approach, combined with experimental spectroscopic data, may provide a non-destructive, facile route for the rapid evaluation of impact sensitivity of small-scale (mg) samples of novel EMs that can differentiate between highly sensitive and insensitive compounds. With further developments of our up-pumping model theory, we plan to extend our test set to a broader range of EMs, including multi-component materials, in follow up investigations.

Although such a spectroscopic method will not replace more accurate and well-established drop-weight impact testing, we propose that lab-based THz-Raman spectroscopy could become an important diagnostic technique to evaluate sensitivity, thereby informing the safety precautions required for subsequent scale up of synthetic procedures. Such an approach is likely to expedite the design and discovery of new EMs.

## Conflicts of interest

There are no conflicts to declare.

## Data availability

Processed data are available in supplementary information (SI). Supplementary information: DFT simulated frequencies. See DOI: <https://doi.org/10.1039/d5cp03040d>.

Raw INS data are available from the data repository of the ISIS Neutron and Muon Facility (<https://data.isis.stfc.ac.uk/datagateway>).

## Acknowledgements

INS data were collected in proposal RB1710382. Computations were performed using the University of Birmingham's BlueBEAR HPC service, which provides a High-Performance Computing service to the University's research community. Computations were also performed through the Young super-computer, *via* the UK's Materials and Molecular Modelling Hub, which is partially funded by EPSRC (EP/T022213/1)

## Notes and references

- 1 D. Mathieu, *Ind. Eng. Chem. Res.*, 2017, **56**, 8191–8201.
- 2 D. Mathieu, *J. Phys. Chem. A*, 2013, **117**, 2253–2259.
- 3 V. Prana, G. Fayet, P. Rotureau and C. Adamo, *J. Hazard. Mater.*, 2012, **235–236**, 169–177.
- 4 H. M. Quayle, K. Mohan, S. Seth, C. R. Pulham and C. A. Morrison, *Digital Discovery*, 2025, **4**, 3260–3269.
- 5 N. Lease, L. M. Klamborowski, R. Perriot, M. J. Cawkwell and V. W. Manner, *J. Phys. Chem. Lett.*, 2022, **13**, 9422–9428.
- 6 Q. Deng, J. Hu, L. Wang, Y. Liu, Y. Guo, T. Xu and X. Pu, *Chemom. Intell. Lab. Syst.*, 2021, **215**, 104331.
- 7 B. M. Rice and J. J. Hare, *J. Phys. Chem. A*, 2002, **106**, 1770–1783.
- 8 J. S. Murray, M. C. Concha and P. Politzer, *Mol. Phys.*, 2009, **107**, 89–97.
- 9 B. Asay, B. Henson, L. Smilowitz and P. M. Dickson, *J. Energ. Mater.*, 2003, **21**, 223–235.
- 10 O. Bolton, L. R. Simke, P. F. Pagoria and A. J. Matzger, *Cryst. Growth Des.*, 2012, **12**, 4311–4314.
- 11 L. E. Fried and A. J. Ruggiero, *J. Phys. Chem.*, 1994, **98**, 9786–9791.
- 12 D. D. Dlott and M. D. Fayer, *J. Chem. Phys.*, 1990, **92**, 3798–3812.
- 13 D. D. Dlott, *Advanced Series in Physical Chemistry*, WORLD SCIENTIFIC, 2005, vol. 16, pp. 303–333.
- 14 A. A. L. Michalchuk, S. Rudić, C. R. Pulham and C. A. Morrison, *Phys. Chem. Chem. Phys.*, 2018, **20**, 29061–29069.
- 15 A. A. L. Michalchuk, *Faraday Discuss.*, 2023, **241**, 230–249.
- 16 A. A. L. Michalchuk, J. Hemingway and C. A. Morrison, *J. Chem. Phys.*, 2021, **154**, 064105.
- 17 J. M. Hemingway, H. M. Quayle, C. Byrne, C. R. Pulham, S. Mondal, A. A. L. Michalchuk and C. A. Morrison, *Phys. Chem. Chem. Phys.*, 2025, **27**, 11640.
- 18 J. Bernstein, *J. Chem. Phys.*, 2018, **148**, 084502.
- 19 X. Bidault and S. Chaudhuri, *RSC Adv.*, 2022, **12**, 31282–31292.
- 20 A. A. L. Michalchuk, S. Rudić, C. R. Pulham and C. A. Morrison, *Chem. Commun.*, 2021, **57**, 11213–11216.
- 21 I. L. Christopher, C. R. Pulham, A. A. L. Michalchuk and C. A. Morrison, *J. Chem. Phys.*, 2023, **158**, 124115.
- 22 I. L. Christopher, X. Liu, H. J. Lloyd, C. L. Bull, N. P. Funnell, P. Portius, A. A. L. Michalchuk, S. R. Kennedy, C. R. Pulham



- and C. A. Morrison, *Phys. Chem. Chem. Phys.*, 2024, **26**, 16859–16870.
- 23 R. L. Simpson, P. A. Urtiew, D. L. Ornellas, G. L. Moody, K. J. Scribner and D. M. Hoffman, *Propellants, Explos., Pyrotech.*, 1997, **22**, 249–255.
- 24 C. B. Storm, J. R. Stine and J. F. Kramer, in *Chemistry and Physics of Energetic Materials*, ed. S. N. Bulusu, Springer Netherlands, Dordrecht, 1990, pp. 605–639.
- 25 J. A. Spies, J. Neu, U. T. Tayvah, M. D. Capobianco, B. Pattengale, S. Ostresh and C. A. Schmuttenmaer, *J. Phys. Chem. C*, 2020, **124**, 22335–22346.
- 26 N. Menchu and A. K. Chaudhary, *J. Opt. Photonics Res.*, DOI: [10.47852/bonviewJOPR52024465](https://doi.org/10.47852/bonviewJOPR52024465).
- 27 H. Huang, Z. Liu, M. T. Ruggiero, Z. Zheng, K. Qiu, S. Li, Z. Zhang and Z. Zhang, *Cryst. Growth Des.*, 2025, **25**, 3578–3594.
- 28 M. W. S. Chong, M. R. Ward, C. McFarlan, A. J. Parrott, P. Dallin, J. Andrews, I. D. H. Oswald and A. Nordon, *Chem. Commun.*, 2025, **61**, 925–928.
- 29 M. D. King, W. D. Buchanan and T. M. Korter, *Anal. Chem.*, 2011, **83**, 3786–3792.
- 30 J. T. A. Carriere, F. Havermeier and R. A. Heyler, THz-Raman spectroscopy for explosives, chemical and biological detection, in *Proceedings of SPIE*, ed. A. W. Fountain, Baltimore, Maryland, USA, 2013, 87100M.
- 31 N. Palka, M. Szala and E. Czerwinska, *Appl. Opt.*, 2016, **55**, 4575.
- 32 A. A. L. Michalchuk, M. Trestman, S. Rudić, P. Portius, P. T. Fincham, C. R. Pulham and C. A. Morrison, *J. Mater. Chem. A*, 2019, **7**, 19539–19553.
- 33 H. Kim and D. D. Dlott, *J. Chem. Phys.*, 1990, **93**, 1695–1709.
- 34 P. Virtanen, R. Gommers, T. E. Oliphant, M. Haberland, T. Reddy, D. Cournapeau, E. Burovski, P. Peterson, W. Weckesser, J. Bright, S. J. Van Der Walt, M. Brett, J. Wilson, K. J. Millman, N. Mayorov, A. R. J. Nelson, E. Jones, R. Kern, E. Larson, C. J. Carey, Í. Polat, Y. Feng, E. W. Moore, J. VanderPlas, D. Laxalde, J. Perktold, R. Cimrman, I. Henriksen, E. A. Quintero, C. R. Harris, A. M. Archibald, A. H. Ribeiro, F. Pedregosa, P. Van Mulbregt, SciPy 1.0 Contributors, A. Vijaykumar, A. P. Bardelli, A. Rothberg, A. Hilboll, A. Kloeckner, A. Scopatz, A. Lee, A. Rokem, C. N. Woods, C. Fulton, C. Masson, C. Häggström, C. Fitzgerald, D. A. Nicholson, D. R. Hagen, D. V. Pasechnik, E. Olivetti, E. Martin, E. Wieser, F. Silva, F. Lenders, F. Wilhelm, G. Young, G. A. Price, G.-L. Ingold, G. E. Allen, G. R. Lee, H. Audren, I. Probst, J. P. Dietrich, J. Silterra, J. T. Webber, J. Slavič, J. Nothman, J. Buchner, J. Kulick, J. L. Schönberger, J. V. De Miranda Cardoso, J. Reimer, J. Harrington, J. L. C. Rodríguez, J. Nunez-Iglesias, J. Kuczynski, K. Tritz, M. Thoma, M. Newville, M. Kümmerer, M. Bolingbroke, M. Tartre, M. Pak, N. J. Smith, N. Nowaczyk, N. Shebanov, O. Pavlyk, P. A. Brodtkorb, P. Lee, R. T. McGibbon, R. Feldbauer, S. Lewis, S. Tygier, S. Sievert, S. Vigna, S. Peterson, S. More, T. Pudlik, T. Oshima, T. J. Pingel, T. P. Robitaille, T. Spura, T. R. Jones, T. Cera, T. Leslie, T. Zito, T. Krauss, U. Upadhyay, Y. O. Halchenko and Y. Vázquez-Baeza, *Nat. Methods*, 2020, **17**, 261–272.
- 35 R. A. Heyler, J. T. A. Carriere and F. Havermeier, *Proc. SPIE* 8926, Next-Generation Spectroscopic Technologies VI, 87260J, Baltimore, 2013.
- 36 K. L. McNesby and C. S. Coffey, *J. Phys. Chem. B*, 1997, **101**, 3097–3104.

